

# OBSERVED SPECTRAL INVARIANT BEHAVIOR OF ZENITH RADIANCE IN THE TRANSITION ZONE BETWEEN CLOUD-FREE AND CLOUDY REGIONS

A. Marshak<sup>1</sup>, Y. Knyazikhin<sup>2</sup>, C. Chiu<sup>3</sup>, and W. Wiscombe<sup>1</sup>

<sup>1</sup>NASA Goddard Space Flight Center, Greenbelt, MD, USA

<sup>2</sup>Boston University, Boston, MA, USA

<sup>3</sup>Joint Center for Earth Systems Technology, UMBC, Baltimore, MD, USA

## ABSTRACT

The Atmospheric Radiation Measurement Program's (ARM) new Shortwave Spectrometer (SWS) looks straight up and measures zenith radiance at 418 wavelengths between 350 and 2200 nm. Because of its 1-sec sampling resolution, the SWS provides a unique capability to study the transition zone between cloudy and clear sky areas. A surprising spectral invariant behavior is found between ratios of zenith radiance spectra during the transition from cloudy to cloud-free atmosphere. This behavior suggests that the spectral signature of the transition zone is a linear mixture between the two extremes (definitely cloudy and definitely clear). The weighting function of the linear mixture is found to be a wavelength-independent characteristic of the transition zone. It is shown that the transition zone spectrum is fully determined by this function and zenith radiance spectra of clear and cloudy regions. This new finding may help us to better understand and quantify such physical phenomena as humidification of aerosols in the relatively moist cloud environment and evaporation and activation of cloud droplets.

**Index Terms** — ARM, spectral radiance, cloud-free to cloud transition zone

## 1. OBSERVATIONS

Figure 1 shows a 300 s segment of normalized spectral zenith radiances measured by SWS on 18 May 2007 at the ARM SGP site. The vertical axis shows wavelength from 350 to 2170 nm. Strong water vapor absorption bands are seen at wavelengths of 930, 1120, 1400, and 1900 nm. Based on the color palette, we can roughly identify the first 60 s as clear followed by 120 s of cloudy and then by 120 s of clear. The wind speed of 3 m/s at cloud-base height of 2.0 km (derived from the ARM wind profiler) converts the observation time of 300 s into 900 m with a cloud diameter of roughly 360 m. Cloud top height was found at 2.1 km by lidar and radar, so the cloud was only 100 m thick. Four

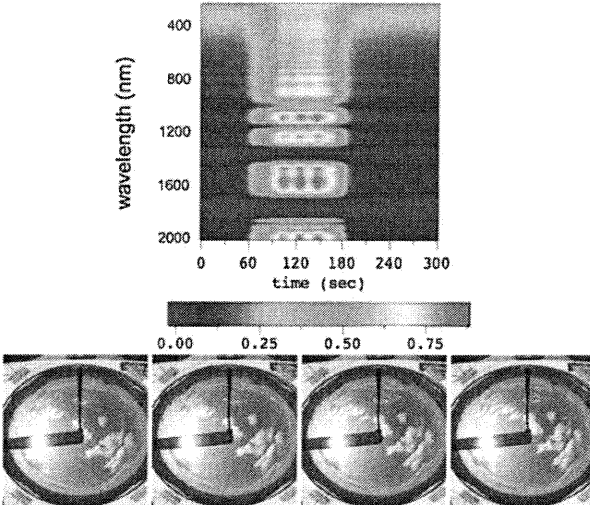


**Figure 1.** *Top:* time-wavelength color contour plot of ARM SWS spectra measured from 21:35:24 to 21:40:24 UTC on 18 May 2007 at ARM SGP site in Oklahoma. SZA = 450. SWS-observed zenith radiances have been normalized by  $\cos(\text{SZA})$  and by the extraterrestrial solar spectrum. *Bottom:* four total-sky images taken at 21:38:00 (156 s), and 21:38:30 (186 s), 21:39:00 (216 s) and 21:39:30 (246 s) during the time when the small cloud at zenith was moving from inside to outside the field of view of the SWS. From [1].

total sky images taken 30 s apart starting from 156 s indicate that the cloud moves toward the northeast.

Let  $t_0$  be the time corresponding to the cloud edge. We choose  $t_0 = 150$  s for our example (see Figure 1). Let  $t_T$  denote the time of definitely clear observations. The length of transition zone,  $T = t_T - t_0$ , is 100 s in our analysis. With a wind speed of 3 m/s,  $T$  corresponds to a 300 m spatial segment. Figure 2 illustrates the normalized zenith radiance spectrum,  $I(t, \lambda)$ , plotted at 10 s time intervals from  $t_0 = 150$  s to  $t_T = 250$  s.

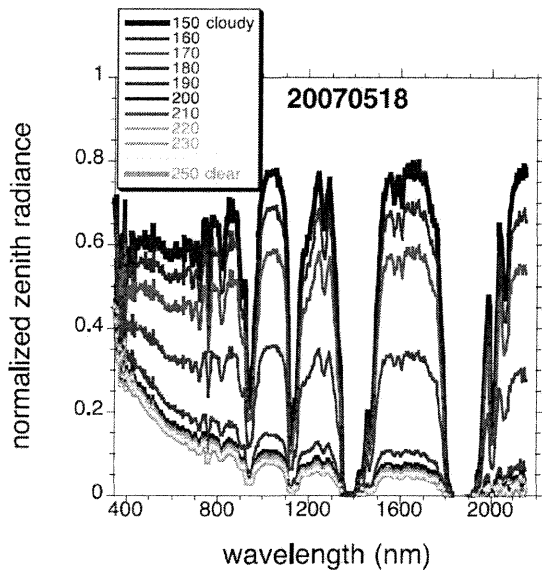


**Figure 2.** Normalized SWS zenith radiance spectrum,  $I(t, \lambda)/I(T, \lambda)$ , measured on 18 May 2007 from  $t_0 = 150$  s (cloudy) to  $t_T = 250$  s (clear) with 10 s time interval. Same case as Figure 1. From [1].

Figure 3 plots values of spectrum  $I(t, \lambda)/I(T, \lambda)$  vs.  $I(t_0, \lambda)/I(T, \lambda)$  for 9 values of time  $t$  between 160 s and 250 s. The upper panel demonstrates relationships using data from 350 to 1800 nm while the lower panel shows just the visible spectral interval. Very high values of the linear regression coefficient suggest a nearly perfect linear variation with slope  $a(t)$  and intercept  $b(t)$  adding up to unity with 2–5% uncertainties (at 190 s the sum deviated most from unity, 1.08). Clearly, the linear relationship does not depend on wavelength, and thus  $a(t)$  does not depend on wavelength.

It is not surprising that  $a(t) + b(t) = 1$ . Indeed, as  $\lambda$  goes toward UV wavelengths where Rayleigh scattering increasingly dominates cloud scattering, the difference between clear and cloudy zenith radiance becomes smaller (see Figures 1 and 2) and  $I(t, \lambda) \approx I(t_0, \lambda) \approx I(T, \lambda)$ . As a result, equation (4) leads to  $a(t) + b(t) \approx 1$ .

It follows from these empirical results that the spectral signature,  $I(t, \lambda)$ , of the transition zone is a linear mixture between the two extremes (definitely cloudy and definitely clear). The weighting function of the linear mixture is a wavelength-independent characteristic of the transition zone. The transition zone spectrum is fully determined by this function and zenith radiance spectra of clear and cloudy regions. More details can be found in [1].

## 2. DISCUSSIONS

Spectral invariant behavior found in the transition zone between cloudy and cloud-free areas is surprising. In

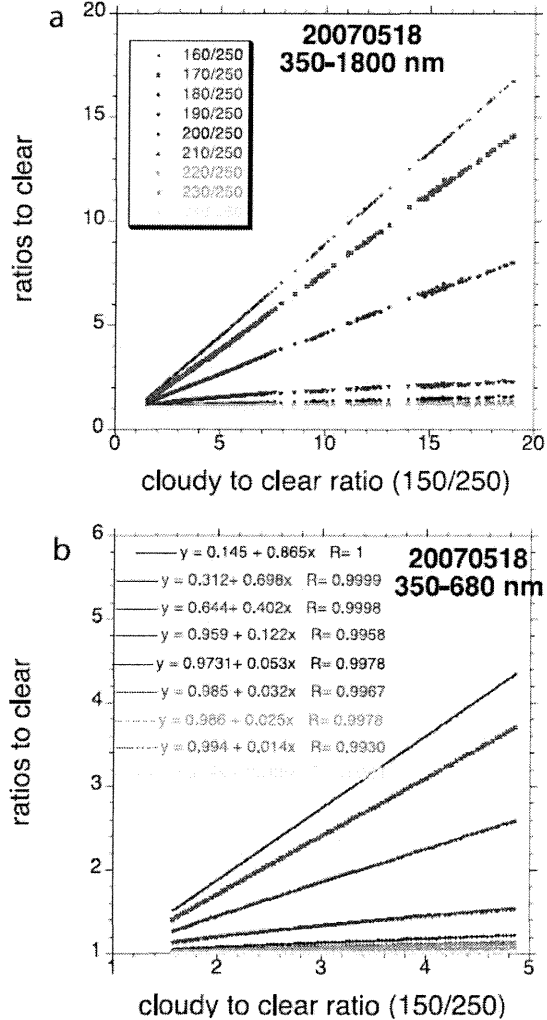


**Figure 3.** Ratio  $I(t, \lambda)/I(T, \lambda)$  vs. ratio  $I(t_0, \lambda)/I(T, \lambda)$  for 9 values of time from  $t = 160$  s to  $t = 240$  s with linear fit and the coefficients of linear regression. (a) Wavelengths from 350 to 1800 nm. (b) Wavelengths from 350 nm to 680 nm. 18 May 2007 case of Figure 1. To avoid division by small numbers (see Figure 2) we excluded these strong water vapor absorbing spectral intervals: 931–970 nm, 1087–1164 nm, 1301–1495 nm, and 1800–1960 nm. We have also masked spectral measurements at wavelengths longer than 2000 nm because the clear sky values of zenith radiance at these wavelengths are too low and too uncertain to be used as a denominator in the ratios. From [1]

vegetation canopy, linear relationships between some algebraic combinations of measured reflectance, transmittance and absorptance of shortwave spectra have recently been observed and physics behind such phenomena

have been documented [2-5]. The slope and intercept of the relationships are indicative of canopy micro- and macroproperties [6-8]. The independency of the interaction cross-section on wavelength was critical to explain spectrally invariant behavior in the case of vegetation canopy. In the atmosphere this condition is not met and thus the physics behind the observed spectral signature of the transition zone between cloudy and clear sky areas remains unexplained. Search for similar phenomena in clouds and understanding of their physics are essential to better understanding of cloud observations since it allows separation of the structural and radiometric components of measured signal.

### 3. ACKNOWLEDGMENTS

This research is supported by the Office of Science (BER, U.S. Department of Energy, Interagency Agreements DEAI02-08ER64562, DE-FG02-08ER64563, and DE-FG02-08ER54564) as part of the US DoE Atmospheric Radiation Measurement Program program

### 4. REFERENCES

- [1] A. Marshak, Y.Knyazikhin, J.C. Chiu, and W. Wiscombe, "Spectral invariant behavior of zenith radiance around cloud edges observed by ARM SWS," *Geophys. Res. Lett.*, 36, L16802, doi:10.1029/ 2009GL039366 (2009).
- [2] Y. Knyazikhin, A. Marshak, and R.B. Myneni, "Three-Dimensional Radiative Transfer in Vegetation Canopies and Cloud-Vegetation Interaction," A. Marshak and A.B. Davis [Eds.], *Three Dimensional Radiative Transfer in the Cloudy Atmosphere*, Springer-Verlag, pp. 617-652 (2005).
- [3] O. Panferov, Y. Knyazikhin, R.B. Myneni, J. Szarzynski, S. Engwald, K.G. Schnitzler, and G. Gravenhorst, "The role of canopy structure in the spectral variation of transmission and absorption of solar radiation in vegetation canopies," *IEEE Trans. Geosci. and Rem. Sens.*, 39, pp. 241–253 (2001).
- [4] D. Huang, Y. Knyazikhin, R. E. Dickinson, M. Rautiainen, P. Stenberg, M. Disney, P. Lewis, A. Cescatti, Y. Tian, W. Verhoef, J. V. Martonchik, and R. B. Myneni, "Canopy spectral invariants for remote sensing and model applications," *Remote Sens. Environ.*, 106, pp. 106-122 (2007).
- [5] Y. Knyazikhin, M. A. Schull and L. Xu, "Canopy spectral invariants: a new concept in remote sensing of vegetation," *Journal of Quantitative Spectroscopy & Radiative Transfer*, submitted, January, 2010.
- [6] S. Smolander and P. Stenberg, "Simple parameterizations of the radiation budget of uniform broadleaved and coniferous canopies," *Remote Sens. Environ.*, 94, pp. 355–363 (2005).
- [7] P. Lewis and M. Disney, "Spectral invariants and scattering across multiple scales from within-leaf to canopy," *Remote Sens. Environ.*, 109, pp. 196-206 (2007).
- [8] M. A. Schull, L. Xu, A. Samanta, S. Ganguly, P. L. Carmona, J. P. Jenkins, L. Plourde, Y. Knyazikhin, and R. B. Myneni, "Canopy spectral invariants: a theoretical basis for classification of forest types from hyperspectral data," *J. Quantitative Spectroscopy & Radiative Transfer*, submitted, January, (2010).